All-fiber-based laser with 200 mHz linewidth

Junchao Huang (黄军超)[1,2], Lingke Wang (汪凌珂)[1,2], Yifei Duan (段怡菲)[1,2], Yafeng Huang (黄亚峰)[1,2], Meifeng Ye (叶美凤)[1], Liang Liu (刘 亮)[1], and Tang Li (李 唐)[1,*]

[1]*Key Laboratory of Quantum Optics, Shanghai Institute of Optics and Fine Mechanics, Chinese Academy of Sciences, Shanghai 201800, China*

[2]*Center of Materials Science and Optoelectronics Engineering, University of Chinese Academy of Sciences, Beijing 100049, China*

**Corresponding author: litang@siom.ac.cn*

Received March 1, 2019; accepted April 12, 2019; posted online June 25, 2019

We demonstrate the frequency stabilization of a 1.55 μm erbium-doped fiber laser by locking it to a 5-km-long optical fiber delay line (FDL). The stabilized laser is characterized via comparison with a second identical laser system. We obtain a fractional frequency stability of better than 3×10^{-15} over time scales of 1–10 s and a laser linewidth of 0.2 Hz, which is the narrowest linewidth of an FDL-stabilized laser observed to date.

OCIS codes: 140.3425, 060.2310, 060.2840.
doi: 10.3788/COL201917.071407.

Ultra-stable lasers are required as fundamental tools in the precision measurement science field. A wide variety of applications benefit from the extraordinary spectral purity of these lasers, including optical atomic frequency standards[1–6], high-resolution spectroscopy[7], and fundamental physics tests[8]. State-of-the-art ultra-stable lasers are realized by tightly locking their frequencies to high-finesse Fabry–Pérot (FP) cavities using the Pound–Drever–Hall (PDH) method to reach a fractional frequency stability below 1×10^{-16}[9,10]. To obtain such a high stability, however, special techniques must be used to lower the thermal noise floor, including the use of longer cavities or cryocoolers. These methods dramatically increase the complexity and bulk of the system and consequently limit the transportable applications of ultra-stable lasers. These applications include space optical atomic clocks[11], the Laser Interferometer Space Antenna (LISA) mission for gravitational wave detection[12], ultra-low phase noise microwave synthesizers[13], and optical frequency dissemination[14,15].

A fiber delay line (FDL) has been demonstrated to be a suitable alternative to high-finesse FP cavities for use in laser stabilization[16–18]. In this approach, a heterodyne arm-unbalanced Michelson interferometer is used as a frequency discriminator to extract the laser's frequency fluctuations, which are then fed back to the laser to stabilize its frequency. In contrast to the FP cavity method, this approach can also provide precise and rapid tunability over a wide frequency range, with the exception of the ultra-low frequency noise. This feature is required in many applications, including optical processing of radio-frequency signals[19], optical tracking oscillators[20], coherent light detection and ranging[21], and low-noise interferometric sensors[22]. Recently, a fractional frequency stability of 5×10^{-15}, which is fundamentally limited by the thermomechanical noise in the optical fibers, was demonstrated[18]. In optical fibers, the thermodynamic phase fluctuations of the light include contributions from both thermoconductive noise and thermomechanical noise[23–27]. Thermomechanical noise has a $1/f$ spectral density and is regarded as the fundamental limit of the short-term frequency stability of FDL-stabilized lasers[28]. The influence of this type of noise can be reduced by increasing the length of the unbalanced optical fiber of the interferometer. In this Letter, we demonstrate an ultra-stable laser that is locked to a heterodyne Michelson interferometer using 5-km-long optical fibers, which are 10 times longer than the fibers used in a previous work[18]. This interferometer consequently leads to an improvement of three times in the fractional frequency stability, which is dominated by thermomechanical noise. Additionally, in this work, a vibration-insensitive fiber spool and a multilayer thermal shield are used to improve the laser's isolation from environmental fluctuations. In this way, a stabilized laser with a 200 mHz linewidth and a short-term frequency stability of 2×10^{-15} is achieved.

The experimental setup is shown in Fig. 1. A 1550 nm fiber laser (AdjustiK-E15, NKT Photonics) is used as the laser source. The laser beam is then split into two parts

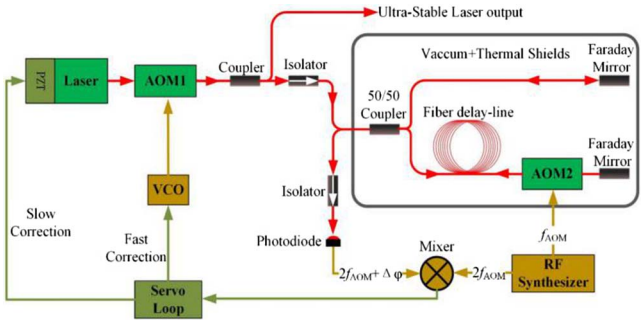

Fig. 1. Experimental setup of the laser stabilization system. PZT: piezoelectric transducer; AOM: acousto-optic modulator; VCO: voltage-controlled oscillator; RF: radio frequency.

using an optical coupler with a coupling ratio of 99∶1. The smaller part (approximately 100 μW) is sent to the interferometer for laser stabilization, passing through an acousto-optic modulator (AOM1), and the larger part is used as the output. The interferometer is an unbalanced fiber Michelson interferometer, and another internal acousto-optic modulator (AOM2) is used to produce a frequency shift (of 80 MHz) for heterodyne detection. The FDL is constructed using a standard single-mode optical fiber (SMF-28, Corning) and has a length of 5 km. The interferometer beat note is detected using a photodiode and is then coherently demodulated to produce an error signal. A proportional-integral circuit then converts this error signal into a laser frequency correction signal. Large-scale dynamic frequency correction is realized via a piezoelectric transducer, while fast frequency correction is provided by a voltage-controlled oscillator, which drives AOM1.

In this scheme, the stabilized laser is sensitive to seismic noise. To resolve this problem, a fiber spool with an ultralow acceleration sensitivity is used. In addition to the low axial acceleration sensitivity, which is similar to the fiber spool in Ref. [29], the radial acceleration sensitivity of this fiber spool has also been optimized. In addition, to isolate the setup from both temperature fluctuations and acoustic noise, the entire interferometer is placed into a vacuum chamber (Fig. 2). The vacuum level is maintained at approximately 3×10^{-5} Pa. The interferometer, with the exception of the AOM, is placed inside three thermal shields. The fiber spool is mounted on the inner shield using Teflon screws, while the other components (i.e., the optical coupler and Faraday mirrors) are fixed in place using low-outgassing epoxy glue. The shields are made from aluminum, and are gold-coated and polished to reduce their emissivity. Additionally, Teflon thermal insulators are used among the fiber spool, the thermal shields, and the vacuum chamber to minimize heat exchanges. AOM2 is mounted flushly against the inner surface of the vacuum chamber because it dissipates heat of approximately 200 mW. This passive shielding can be regarded as a low-pass filter with a time constant of approximately 4.6 days. In addition, the vacuum chamber is temperature stabilized at 27°C using an active thermal controller. The temperature fluctuation is less than 250 μK over a 24 h period.

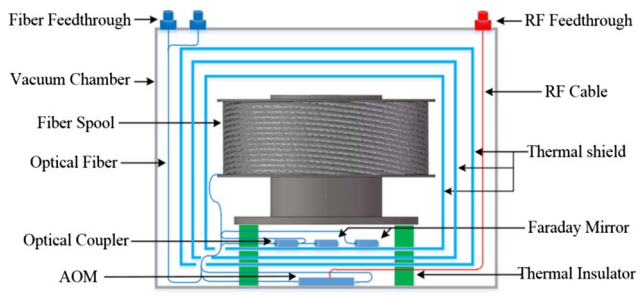

Fig. 2. Schematic of the vacuum chamber.

To evaluate the performance of the stabilized laser setup, we constructed two identical FDL-stabilized laser systems. Each system was constructed using a separate laser source and a separate fiber interferometer. When the output light beams of the two FDL-stabilized laser systems were combined, a heterodyne beat-note signal was detected. One of the merits of FDL-based laser stabilization is the rapid laser frequency tuning capability[17], which provides an easy way to compensate for the inevitable laser frequency drift. A drift of 15 Hz/s was removed by applying a frequency offset to the tunable RF synthesizer. This drift was mainly caused by aging drift of the optical fiber. The residual drift of the measured beat-note signal was less than 0.5 Hz/s. To measure the laser linewidth, the beat-note signal was frequency downconverted to approximately 50 Hz and was then analyzed using a fast Fourier transform (FFT) spectrum analyzer (SR760, Stanford Research Systems). From a series of eighteen consecutive measurements, we obtained a typical full width at half-maximum of 0.28 (0.08) Hz at 0.125 Hz resolution bandwidth (RBW, Fig. 3). The linewidth for a single laser is 0.2 Hz, which is the narrowest linewidth that has been observed for an FDL-stabilized laser to date[16–18].

To measure the laser frequency noise, the RF beat-note signal between the two stabilized lasers (approximately 100 MHz) is sent to a phase noise measurement system (TSC 5125 A, Microsemi) for comparison with a reference signal from an active hydrogen maser (iMaser3000, T4Science) for phase noise measurement. In this measurement, the laser frequency drift is compensated in the same way as the linewidth measurement. The frequency noise power spectral density (PSD) $S_\nu(f)$ is then derived from the phase noise $S_\varphi(f)$ using

$$S_\nu(f) = f^2 S_\varphi(f)\ \mathrm{Hz}^2/\mathrm{Hz}, \tag{1}$$

where f is the Fourier frequency. The measured data are shown in Fig. 4. Curve (a) represents the measured frequency noise of the two lasers and curve (b) represents a theoretical simulation of the fiber thermal noise limit for two 10 km fibers (because light passes through the optical fibers twice in the Michelson scheme). According

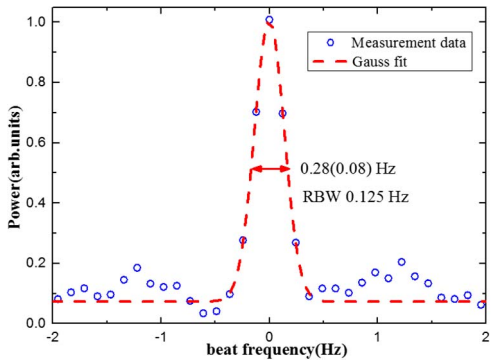

Fig. 3. Normalized FFT spectrum of the beat-note signal (blue circles) and its Gaussian fit (red line).

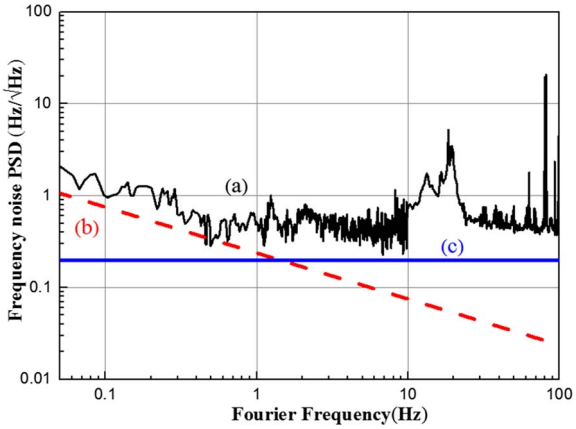

Fig. 4. Frequency noise PSD of (a) two identical FDL-stabilized lasers (black solid line), (b) thermomechanical noise from the optical fiber (red dash line), and (c) thermal noise of the first-stage amplifier after the photodiode (blue solid line).

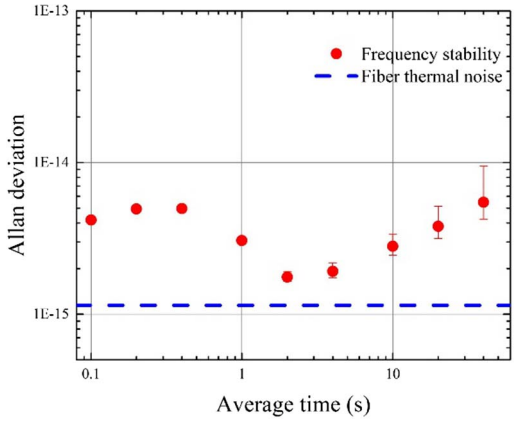

Fig. 5. Fractional frequency instability of FDL-stabilized lasers. The dashed curve denotes the thermomechanical noise limit of the optical fiber.

to thermomechanical noise theory[26], the laser frequency noise PSD that is induced by the fiber thermal noise is given by

$$S_T(f) = \left(\frac{n}{\tau\lambda}\right)^2 \frac{2k_B T L \Phi_0}{3\pi E_0 A f} \ \mathrm{Hz^2/Hz}, \tag{2}$$

where λ is the optical wavelength, τ is the time delay of the FDL, n is the effective refractive index of the optical fiber, k_B is the Boltzmann constant, and T is the temperature; L is the fiber length, $E_0 = 1.9 \times 10^{10}$ Pa is the bulk modulus of the material, $A = 4.9 \times 10^{-8}$ m^2 is the cross-sectional area of the fiber, and $\Phi_0 = 0.01$ is the loss angle of the fiber. Curve (c) represents the thermal noise of the first-stage amplifier after the photodiode. Obviously, the laser frequency noise over the range from 0.05 Hz to 1 Hz is dominated by the fiber's thermomechanical noise, while the thermal noise from the amplifier is the major noise source at the higher Fourier frequencies. The noise bump in the range between 10 Hz and 30 Hz is mainly due to seismic noise and the peaks distributed at the higher Fourier frequencies stem from noises introduced by power-supply grounding such as 50-Hz noise and noises from other electronics devices coupled into the measurement system.

Using the method described above, the frequency fluctuations of the beat-note signal are also recorded every 100 ms. Therefore, through the use of frequency stability analysis software (Stable 32), the fractional frequency stability characteristics of the two lasers can be obtained. The stability of one of the lasers is shown in Fig. 5. The dashed curve at a fractional frequency stability of 1.1×10^{-15} represents the thermomechanical noise limit of the optical fiber. The stability is better than 3×10^{-15} over a timescale of 1–10 s. The instability bump between 0.1 and 1 s is attributed to high-frequency noise, while the rising ramp at time scales above 10 s occurs because of environmental temperature fluctuations or laser intensity fluctuations.

In conclusion, using a 5-km-long optical fiber spool, we have demonstrated an all-fiber-based ultra-stable laser with a linewidth as low as 200 mHz. A fractional frequency stability of less than 5×10^{-15} was achieved over the range from 0.1 s to 40 s. Particularly, at shorter timescales of 2–4 s, the system stability is better than 2×10^{-15}, which is close to the predicted thermomechanical noise floor. In future work, further steps will be taken to improve the stability of the FDL-stabilized laser and minimize the system overall: (1) better stabilization of the laser intensity will be required to achieve optimal long-term stability; (2) an optical fiber with lower mechanical loss will be used to reduce the thermomechanical noise floor[28]; (3) an ultra-low vibration sensitivity fiber spool that is smaller in size[30] or the feedforward method[31] will be used to allow the FDL-stabilized lasers to operate without vibration isolation platforms and will thus make them more compact.

This work was supported by the National Natural Science Foundation of China (NSFC) (Nos. 11604353, 11274324, and 11704391) and the Key Research Program of the Chinese Academy of Sciences (No. KJZD-EW-W02).

References

1. A. D. Ludlow, M. M. Boyd, J. Ye, E. Peik, and P. O. Schmidt, Rev. Mod. Phys. **87**, 637 (2015).
2. I. Ushijima, M. Takamoto, M. Das, T. Ohkubo, and H. Katori, Nat. Photonics **9**, 185 (2015).
3. N. Huntemann, C. Sanner, B. Lipphardt, C. Tamm, and E. Peik, Phy. Rev. Lett. **116**, 063001 (2016).
4. S. L. Campbell, R. B. Hutson, G. E. Marti, A. Goban, N. Darkwah Oppong, R. L. McNally, L. Sonderhouse, J. M. Robinson, W. Zhang, B. J. Bloom, and J. Ye, Science **358**, 90 (2017).
5. Y. Li, Y. G. Lin, Q. Wang, T. Yang, Z. Sun, E. J. Zang, and Z. J. Fang, Chin. Opt. Lett. **16**, 051402 (2018).
6. X. H. Fu, S. Fang, R. C. Zhao, Y. Zhang, J. C. Huang, J. F. Sun, Z. Xu, and Y. Z. Wang, Chin. Opt. Lett. **16**, 060202 (2018).

7. W. H. Oskay, W. M. Itano, and J. C. Bergquist, Phys. Rev. Lett. **94**, 163001 (2005).
8. C. Eisele, A. Y. Nevsky, and S. Schiller, Phys. Rev. Lett. **103**, 090401 (2009).
9. S. Häfner, S. Falke, C. Grebing, S. Vogt, T. Legero, M. Merimaa, C. Lisdat, and U. Sterr, Opt. Lett. **40**, 2112 (2015).
10. D. G. Matei, T. Legero, S. Häfner, C. Grebing, R. Weyrich, W. Zhang, L. Sonderhouse, J. M. Robinson, J. Ye, F. Riehle, and U. Sterr, Phys. Rev. Lett. **118**, 263202 (2017).
11. S. Schiller, A. Görlitz, A. Nevsky, S. Alighanbari, S. Vasilyev, C. Abou-Jaoudeh, G. Mura, T. Franzen, U. Sterr, S. Falke, Ch. Lisdat, E. Rasel, A. Kulosa, S. Bize, J. Lodewyck, G. M. Tino, N. Poli, M. Schioppo, K. Bongs, Y. Singh, P. Gill, G. Barwood, Y. Ovchinnikov, J. Stuhler, W. Kaenders, C. Braxmaier, R. Holzwarth, A. Donati, S. Lecomte, D. Calonico, and F. Levi, in *Proceedings of European Frequency and Time Forum* (IEEE, 2012), p. 412.
12. K. Döringshoff, K. Möhle, M. Nagel, E. V. Kovalchuk, and A. Peters, in *Proceedings of European Frequency and Time Forum* (IEEE, 2010), p. 1.
13. T. M. Fortier, M. S. Kirchner, F. Quinlan, J. Taylor, J. C. Bergquist, T. Rosenband, N. Lemke, A. D. Ludlow, Y. Y. Jiang, C. W. Oatesand, and S. A. Diddamset, Nat. Photonics **5**, 425 (2011).
14. O. Lopez, A. Haboucha, F. Kéfélian, H. F. Jiang, B. Chanteau, V. Roncin, C. Chardonner, A. Amy-Klein, and G. Santarelli, Opt. Express **18**, 16849 (2010).
15. C. Q. Ma, L. F. Wu, Y. Y. Jiang, H. F. Yu, Z. Y. Bi, and L. S. Ma, Appl. Phys. Lett. **107**, 261109 (2015).
16. F. Kéfélian, H. F. Jiang, P. Lemonde, and G. Santarelli, Opt. Lett. **34**, 914 (2009).
17. H. F. Jiang, F. Kéfélian, P. Lemonde, A. Clairon, and G. Santarelli, Opt. Express **18**, 3284 (2010).
18. J. Dong, Y. Q. Hu, J. C. Huang, M. F. Ye, Q. Z. Qu, T. Li, and L. Liu, Appl. Opt. **54**, 1152 (2015).
19. V. Lavielle, I. Lorgeré, J. L. Le Gouët, S. Tonda, and D. Dolfi, Opt. Lett. **28**, 384 (2003).
20. P. Wolf, C. J. Bordé, A. Clairon, L. Duchayne, A. Landragin, P. Lemonde, G. Santarelli, W. Ertmer, E. Rasel, F. S. Cataliotti, M. Inguscio, G. M. Tino, P. Gill, H. Klein, S. Reynaud, C. Salomon, E. Peik, O. Bertolami, P. Gil, J. Páramos, C. Jentsch, U. Johann, A. Rathke, P. Bouyer, L. Cacciapuoti, D. Izzo, P. Natale, B. Christophe, P. Touboul, S. G. Turyshev, J. Anderson, M. E. Tobar, F. Schmidt-Kaler, J. Vigué, A. A. Madej, L. Marmet, M.-C. Angonin, P. Delva, P. Tourrenc, G. Metris, H. Müller, R. Walsworth, Z. H. Lu, L. J. Wang, K. Bongs, A. Toncelli, M. Tonelli, H. Dittus, C. Lämmerzahl, G. Galzerano, P. Laporta, J. Laskar, A. Fienga, F. Roques, and K. Sengstock, Exp. Astron. **23**, 651 (2009).
21. M. Harris, G. N. Pearson, J. M. Vaughan, D. Letalick, and C. Karlsson, J. Mod. Opt. **45**, 1567 (1998).
22. J. Hough and S. Rowan, J. Opt. A **7**, S257 (2005).
23. W. H. Glenn, IEEE J. Quantum Electron. **25**, 1218 (1989).
24. K. H. Wanser, Electron. Lett. **28**, 53 (1992).
25. S. Foster, A. Tikhomirov, and M. Milnes, IEEE J. Quantum Electron. **43**, 378 (2007).
26. L. Z. Duan, Electron. Lett. **46**, 1515 (2010).
27. L. Z. Duan, Phys. Rev. A **86**, 023817 (2012).
28. J. Dong, J. C. Huang, T. Li, and L. Liu, Appl. Phys. Lett. **108**, 021108 (2016).
29. T. Li, B. Argence, A. Haboucha, H. F. Jiang, J. L. Dornaux, D. Kone, A. Clairon, P. Lemonde, G. Santarelli, C. Nelson, A. Hati, and E. Burt, in *Proceedings of Joint Conference of International Frequency Control Symposium & European Frequency and Time Forum* (IEEE, 2011), p. 1.
30. J. C. Huang, L. K. Wang, Y. F. Duan, Y. F. Huang, M. F. Ye, L. Li, L. Liu, and T. Li, Chin. Opt. Lett. **17**, 081403 (2019).
31. D. R. Leibrandt, J. C. Bergquist, and T. Rosenband, Phys. Rev. A **87**, 023829 (2013).